Dynamic generation of Bell states in a double-quantum-dot array including electron-phonon interaction

L. D. Contreras-Pulido[1,*] and F. Rojas[2]

[1]*Centro de Investigación Científica y de Educación Superior de Ensenada, Apartado Postal 2732, Ensenada, Baja California 22860, Mexico*

[2]*Departamento de Física Teórica, Centro de Ciencias de la Materia Condensada, Universidad Nacional Autónoma de México, Ensenada, Baja California 22800, Mexico*

(Received 13 September 2007; revised manuscript received 11 December 2007; published 3 March 2008)

We demonstrate theoretical stationary and dynamical generation of Bell states in a system of two parallel double quantum dots with one mobile electron each (proposed as two charge qubits) driven by an external potential difference applied to the second of the double dots. For coherent dynamics, it is shown that each one of the four Bell states is obtained through a suitable nonentangled initial condition as well as through the control of the time-dependent external electric field. We analyze dissipative effects on such state formation, due to the coupling with a thermal bath of phonons. Via a Markovian master equation approach, which includes the electron-phonon interaction, we found that Bell-state probabilities are preserved for very low temperature but are adversely affected as the temperature increases. In addition, we include concurrence and charge distribution calculations in order to characterize the double-dot array. This electrostatic mechanism could be of interest in quantum-computation, -information, and -communication schemes.

DOI: 10.1103/PhysRevA.77.032301 PACS number(s): 03.67.Mn, 03.65.Ud, 73.21.La, 73.40.Gk

I. INTRODUCTION

Size reduction in microelectronics and integrated circuits, with the corresponding increase of speed, is approaching a physical limit where quantum effects are present. Since the statement of different quantum algorithms, it has been demonstrated that quantum mechanics offers unexpected possibilities in information transmission and processing [1,2], indicating the potential capabilities of quantum computers for solving problems intractable in a classical computer [1,3,4] and the development of new information and communication protocols.

In quantum-information processing, the basic unit of information, or qubit [1,5,6], is a quantum two-level system in which each state can be used to represent the classical 0 and 1 binary values in such a way that the qubit can also exist in an arbitrary complex superposition of 0 and 1 (inherent quantum parallelism). Each qubit can be entangled with other qubits in order to perform different computing operations [1,5].

Entanglement is one of the central issues under discussion in quantum theory since it serves to distinguish classical and quantum concepts [7]; it is a quantum-mechanical phenomenon in which two or more states are described in reference to each other, even if they are spatially separated, leading to unique correlations between them that are stronger than any classical correlation [8]. The interest in entangled states (defined as nonseparable superpositions of the component states [1,8]) has been recently renewed because they play a role as an important resource for quantum-computation, quantum-communication, and quantum-information techniques [7,9,10]. Among the different kinds of entangled states, the Bell states are the maximally entangled states of two qubits and are very interesting because many quantum-communication schemes such as quantum teleportation [11,12], quantum dense coding [13–15], and quantum cryptography [16] are based on them [1,10,14]; in addition, the understanding of two-particle entanglement can be used as a basis for the generation of states of three or more entangled qubits [17,18].

Mainly motivated by potential applications of entanglement, there is currently great interest in finding ways to create and manipulate entangled states [19–21]. Different physical systems have been proposed for realization of Bell states and their experimental demonstration has been achieved mainly on trapped ions [22–24] and on quantum-optics systems, including, for example, photon polarization states [17,25–27], atom-photon interactions in cavity QED [28,29], and between two spatially separated cavities [30,31].

Solid-state implementation for both qubits and entangled states is very promising because of the inherent scalability for realistic application of quantum computers [3,4] and the relative ease of integration within current technologies [3,4,32–35]. Among such systems, the use of semiconductor quantum dots (QDs) [3,4,36–38] has received increasing attention due to the knowledge of their theoretical and experimental properties and the existence of an industrial base for semiconductor processing. In particular, double quantum dots (DQDs) can be fabricated in a well-controlled way and have been under intense study [39–50], and a charge qubit can be defined through the use of its charge degree of freedom [40,41,49,51]. Such systems offer good control of the qubit via external voltages [45–47].

Realization of Bell states in QDs has been proposed via excitons in a single dot [21,52,53] or in coupled QDs [54,55] as well as in the electronic states in DQDs. Most of these studies refer to two electrons in a single DQD [19,37,42,53] in which electron position and/or spin can be used to define two qubits [37,38,42,56]. In addition, an array of two DQDs

*debora.contreras@icmm.csic.es

with two electrons can be thought of as an array of two charge qubits where entanglement and Bell states are formed [57].

Coherent control of charge in DQDs [45–47] and even experimental demonstration of entanglement [58] have been achieved by means of an external electric field. Thus, these systems have also been theoretically considered for Bell-state creation and control [19,37,42,57,58].

However, one of the major obstacles to solid-state implementations of qubits [1,48,59,60] and entanglement [24] is the decoherence caused by the interaction of the system with the environment, which inevitably disturbs the desired quantum evolution of a quantum-information process. For such quantum-dot realization, loss of coherence is mainly due to interaction with acoustic phonons [53,59,61–63]. Dissipation in qubits based on DQDs has been theoretically studied in different ways, including, for example, phenomenological calculations using a damping parameter in the equations of motion [64], stochastic equations for the population differences and dipole moments of the DQDs [65], and also by means of microscopic models. In particular, the latter have taken into account dissipative effects in formation of Bell states for both diagonal [53,56] and nondiagonal [42,57,66,67] electron-phonon interaction.

The quantification of the degree to which a system is entangled is also an important task, and the theory of quantum entangled states is based on entanglement measures, which are scalar quantities that quantify quantum correlations and distinguish them from classical ones [7]. For bipartite pure states these measures exist and are straightforward to compute [2,7]. On the other hand, for systems that are in a statistical mixture (or mixed states), as observed in realistic experiments, there are also different proposed measures (such as the von Neumann entropy, entanglement of formation, and distillable entanglement, among others) but these cannot be effectively computed for a generic mixed state [2,7] and only a few exceptions are well known, like Wootters' expression for the "concurrence" of two qubits [68].

Here, we theoretically explore the formation and control of entangled states in an array of two parallel DQDs in terms of a static and dynamic external applied potential V_a. Each DQD has one extra electron, which by means of tunneling events can be in the upper or lower dot [see Fig. 1(a)], acting as the states of a charge qubit. Thus, in practice, we have an array of two charge qubits while the external potential can represent variations in the quantum-dot operation, dot size, and even the input of a computational process. This theoretical DQD configuration is close to one realized in recent experiments where Coulomb interaction between two DQDs is analyzed [69].

The main purpose of this paper lies in the demonstration of coherent dynamic formation and control of each one of the Bell states through the control of the time-dependent external potential. Bell states can be related to charge distribution states in the DQD array, as explained below and as shown in Fig. 1(b).

By means of the coupling of the charge qubits with a thermal bath of phonons, dissipation is also considered through a microscopic model for nondiagonal electron-phonon interactions. To this end, we use a quantum open

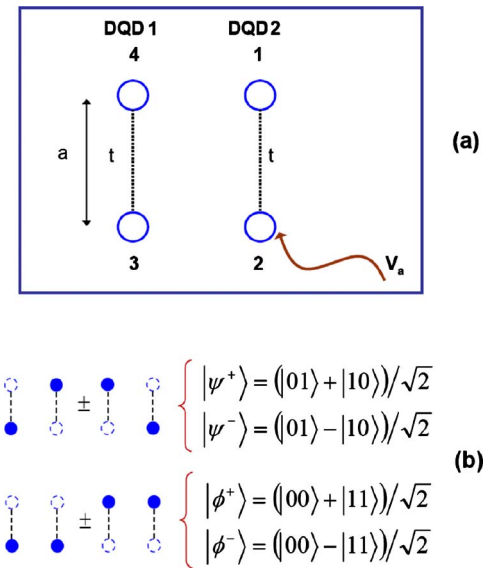

FIG. 1. (Color online) (a) Two double quantum dots in a square geometry with an external potential difference applied in the second quantum dot. Each double dot has one extra electron and tunneling is allowed only vertically. (b) The four Bell states related to charge distribution inside the array.

system approach for the study of the dynamical evolution of the reduced density matrix of the system, and we evaluate the effects of temperature on charge distribution, concurrence, and Bell-state probabilities in the DQD array.

Wootters' concurrence is used to characterize the degree of entanglement in our system, for both pure and mixed states. On the other hand, charge distribution is quantified via the "polarization" [64,70] which refers to the electron localization in opposite quantum dots inside the array [see Eq. (10) below].

In particular, we find that each Bell state can be obtained in this qubit array with the largest probability, through the control of a time-dependent external electric potential and from specific initial nonentangled charge states. Bell states can be maintained for very low temperatures, but they deteriorate as the temperature increases, and we observe that the system loses any quantum correlation for finite (or critical) temperature, which for the typical tunneling used here is around 2.75 K.

The paper is organized as follows. In Sec. II we present the general model used in this study. With an extended Hubbard-type Hamiltonian, the Coulomb interactions in the charge-qubit array as well as the driving electric potential are described. The thermal bath is modeled by a set of harmonic oscillators, and a nondiagonal electron-phonon coupling is considered in a way that represents phonon emission and absorption due to electron tunneling inside the QD array. By a numerical diagonalization of the isolated array with a static electric potential, the stationary behavior of the charge distribution and entangled state formation are calculated for the ground state. For a time-dependent potential, the coherent dynamics of the density matrix for the isolated array is obtained from the Liouville equation, whereas for dissipative dynamics we derived a Markovian master equation for the

time evolution of the reduced density operator. The results obtained from these three studies are presented in Sec. III, where concurrence, polarization, and Bell-state probabilities are shown as functions of the relevant parameters of the system with emphasis on the coherent dynamics of each Bell-state formation (from uncorrelated initial states) and on the effects of temperature on both concurrence behavior and probability for each Bell state. Finally, we summarize and conclude in Sec. IV.

II. MODEL

We have an array of two parallel double quantum dots with one extra electron each, arranged in a square geometry and coupled by Coulomb interactions, representing two coupled charge qubits. This array is described by an extended Hubbard-type Hamiltonian [66,67]:

$$H_S = \sum_i \varepsilon_i \hat{n}_i + t\sum_{\langle ij\rangle} (\hat{c}_i^\dagger \hat{c}_j + \hat{c}_j^\dagger \hat{c}_i) + \sum_{i>j} V_{ij}\hat{n}_i\hat{n}_j, \tag{1}$$

where $\hat{c}_i^\dagger$ ($\hat{c}_i$) is the creation (annihilation) operator for electrons, $\hat{n}_i = \hat{c}_i^\dagger \hat{c}_i$ is the electron number operator, and ε_i is the on-site energy at the ith quantum dot. The Coulomb interaction between electrons in dots i and j separated by a distance d_{ij} is $V_{ij} = V/d_{ij}$, and the electron tunneling amplitude between nearest-neighbor dots $\langle ij\rangle$ is t (not to be confused with the time); for our specific case tunneling is allowed only vertically as shown in Fig. 1(a). The electric potential difference V_a is applied only on the second DQD configuration, Fig. 1(a). Note that its effect on the QD system is a shift in the energy of the second quantum dot, that is, ε_2 is renormalized with the potential as $\varepsilon_2 + V_a$, which is the energy used in the calculations for this site. We consider spinless electrons, and double occupancy is forbidden.

For dissipative dynamics, the open system is described by the total Hamiltonian $H = H_S + H_R + V_{SR}$ where the subscripts S and R stand for the system (DQD configuration) and the reservoir (or bath), respectively. We consider a dissipative model like the one used in Ref. [66], in which the thermal bath of phonons is given by a set of harmonic oscillators of frequency ω_k, $H_R = \Sigma_k \hbar\omega_k b_k^\dagger b_k$, where $b_k^\dagger$ (b_k) are the creation (annihilation) phonon operators.

The electron-phonon interaction is given by

$$V_{SR} = \sum_k \sum_{jj'} \alpha_{kjj'} \hat{c}_j^\dagger \hat{c}_{j'} (b_k^\dagger + b_k), \tag{2}$$

which corresponds to absorption or emission of a phonon for electron tunneling events, with matrix elements given by the coefficients $\alpha_{kjj'} = D g_k(\omega_k)$, where $g_k(\omega_k) \propto \omega_k^{1/2}$ describes the frequency-dependent amplitude of the interaction and D is the coupling strength constant, both for the deformation potential model. (Although $\alpha_{kjj'}$ depends on both electronic and bosonic properties, the deformation potential is a simple model to describe the coupling, leading to a constant prefactor that does not explicitly depend on the electronic states of the system but encapsulates the key interaction effects [71].)

Notice that, even though the phonons are present everywhere and not only during tunneling events, they yield a uniform on-site energy renormalization in the whole DQD array which will be ignored here. Therefore, just the phonon-assisted tunneling events described by V_{SR} significantly affect the energy levels of the system and thus the dynamics of the array, providing an effective coupling mechanism and allowing energy relaxation processes [67].

As in Refs. [64,67,70], we assume quantum dots with characteristic diameter $\varphi \approx 50$ nm defined on a $GaAs/Al_xGa_{1-x}As$ heterostructure, with an effective mass $m^* = 0.067$. The typical distance between quantum dots is $a \approx 100$ nm, and the dielectric constant of the medium is ≈ 12, yielding an estimated Coulomb repulsion between nearest-neighbor dots of $V \approx 1$ meV, which is taken as the unit of energy in this paper.

For our particular model, the basis is given by the four charge distribution states in the two-DQD array, straightforwardly related to the "computational basis" for two qubits: $|11\rangle = |1\rangle \otimes |1\rangle$, $|10\rangle = |1\rangle \otimes |0\rangle$, $|01\rangle = |0\rangle \otimes |1\rangle$, and $|00\rangle = |0\rangle \otimes |0\rangle$, where 1 (0) represents an electron localized in the upper (lower) QD of each pair, in the order presented in Fig. 1 (the first qubit corresponds to the first DQD—sites 4 and 3—whereas the second qubit includes QDs 1 and 2). Notice that states $|10\rangle$ and $|01\rangle$ correspond to charge located on sites (i.e., QDs) 2 and 4 and 1 and 3, respectively (diagonals of the square defined by the DQDs) and because of electrostatic interaction they have the minimal energy, whereas $|00\rangle$ and $|11\rangle$ states are configurations with both electrons in the bottom (top) sites in each DQD (sides of the square). In this way, Bell states in the computational basis [1] can be directly related to our charge states as shown in Fig. 1(b), where it can be observed that they correspond to linear combinations of charge distributed along both diagonals $[|\Psi^\pm\rangle = (|01\rangle \pm |10\rangle)/2]$ or sides $[|\phi^\pm\rangle = (|00\rangle \pm |11\rangle)/2]$ of the DQD square array.

For the stationary case with a constant potential difference V_a acting on the second DQD and without dissipation, the solution can be found by a direct numerical diagonalization of H_S and we study the ground state properties. For coherent dynamics (no dissipation) a linear time-dependent potential difference is applied in the second DQD, $V_a(t) = -V_{a0}(t - t_0)$ (where V_{a0} is a constant and t_0 is the potential difference response time), and the Liouville–von Neumann equation of motion for the density matrix of the system is solved:

$$\frac{\partial \rho(t)}{\partial t} = -i\hbar[H_S, \rho(t)]. \tag{3}$$

Finally, for dissipative dynamics we start from the time evolution of the total density matrix, given in the interaction picture (I) by

$$\dot{\rho}^{(I)}(t) = -\frac{i}{\hbar}[V_{SR}^{(I)}(t), \rho^{(I)}(0)] - \frac{1}{\hbar}\int_0^t dt'[V_{SR}^{(I)}(t), [V_{SR}^{(I)}(t'), \rho^{(I)}(t')]], \tag{4}$$

where $V_{SR}^{(I)}$ is the array-bath interaction operator [66,67].

We obtain a closed equation for the *reduced density matrix* (RDM), $\rho_S^{(I)}(t) = \mathrm{Tr}_R[\rho^{(I)}(t')]$, where the partial trace is

carried out over the phonon states by using three fundamental assumptions: (i) at all times there exists a stationary reservoir at temperature T with equilibrium density matrix $\rho_R(0)=\exp(-H_R/k_BT)/\mathrm{Tr}_R(-H_R/k_BT)$ (k_B is the Boltzmann constant); (ii) the system S and the reservoir R are initially uncorrelated, implying $\rho^{(I)}(0)=\rho(0)=\rho_S(0)\rho_R(0)$; (iii) the reservoir loses all memory about its interaction with the system in a time much shorter then that needed for the RDM to change appreciably, meaning that $\rho_S^{(I)}(t')\approx\rho_S^{(I)}(t)$ (Markovian approximation). Thus, we arrive at the master equation for the RDM elements [72,73] in the Schrödinger picture and for the instantaneous eigenbasis:

$$\dot{\rho}_S(t)_{ss'}=-i\omega_{ss'}\rho_S(t)_{ss'}+\sum_{m,n}\tilde{\mathbf{R}}_{ss'mn}\rho_S(t)_{mn} \tag{5}$$

where the first term on the right side represents reversible (or coherent) effects which depend on the transition frequencies of the system $\omega_{ss'}=(E_s-E_{s'})/\hbar$ (E_m are the system eigenenergies), while the second term describes relaxation processes (or irreversible dynamics) where $\tilde{\mathbf{R}}_{ss'mn}$ is the relaxation tensor [67,72,73], given explicitly as

$$\tilde{\mathbf{R}}_{ss'mn}=\begin{cases}\delta_{nm}(1-\delta_{ms})\tilde{W}_{sm}-\delta_{ms}\delta_{ns}\sum_{k\neq s}\tilde{W}_{ks} & (s=s'),\\ -\gamma_{ss'}\delta_{ms}\delta_{ns'} & (s\neq s').\end{cases} \tag{6}$$

Here, $\tilde{W}_{nm}$ are the transition rates from state $|m\rangle$ to $|n\rangle$ of the system, which can be expressed in terms of the bath and DQD array properties as

$$\tilde{W}_{mn}=\frac{2\pi}{\hbar^2}D^2|g(\omega_{mn})|^2\mathcal{D}(\omega_{mn})\{|S_{mn}|^2\bar{n}(\omega_{mn})+|S_{mn}|^2[1+\bar{n}(\omega_{mn})]\}, \tag{7}$$

where $\bar{n}(\omega)$ is the mean number of phonons in the reservoir at temperature T (Bose-Einstein distribution), and $\mathcal{D}(\omega)\propto\omega^2$ is the density of phonon states in the Debye model. We have introduced the operator S which represents system electrons interacting with the phonons, Eq. (2). This kind of electron-phonon coupling can be interpreted as phonon-assisted tunneling events. The states involved in such transitions are given in terms of the basis states as $S=|01\rangle\langle 11|+|10\rangle\langle 11|+|01\rangle\langle 00|+|10\rangle\langle 00|$, which, projected onto the instantaneous system eigenbasis, gives the elements S_{mk}. Notice that the first part of this equation ($\propto\bar{n}$) corresponds to phonon absorption while the second ($\propto\bar{n}+1$) corresponds to emission processes, both at a frequency given by the array transition energy ω_{nm} [57,66,67].

The real part of the nonadiabatic parameter $\gamma_{ss'}$ represents the damping rate (loss) of coherence due to the interaction between system and reservoir, which also can be written in terms of the transition rates as $\mathrm{Re}\,\gamma_{ss'}=(\Sigma_{k\neq s}\tilde{W}_{ks}+\Sigma_{k\neq s}\tilde{W}_{ks'})/2$. Its imaginary part represents a shift of the transition frequency $\omega_{ss'}$, which we assume negligible [67,73]. It is also important to note from Eq. (7) that the transition rates satisfy the so-called detailed balance condition [72,73]

$$\frac{\tilde{W}_{nm}}{\tilde{W}_{mn}}=\exp\left(-\frac{\hbar\omega_{nm}}{k_BT}\right). \tag{8}$$

Finally, for a better understanding of the transition rates, we can point out that Eq. (5) for diagonal elements takes the form

$$\dot{\rho}_S(t)_{ss}=\sum_m\tilde{W}_{sm}\rho_S(t)_{mm}-\rho_S(t)_{ss}\sum_m\tilde{W}_{ms}, \tag{9}$$

which means that the probability of having the system state $|s\rangle$ occupied at time t, $\rho_S(t)_{ss}$, increases due to transitions from all other states $|m\rangle$ to $|s\rangle$ [first term in Eq. (9)], and decreases due to transitions from state $|s\rangle$ *to* any state $|m\rangle$ (second term).

Solution of both Eq. (3) for the closed system and the master equation (5) is carried out numerically using a fourth-order Runge-Kutta algorithm, choosing the appropriate integration step in order to ensure that the property $\mathrm{Tr}(\rho_S)=1$ for the RDM is always satisfied.

As we have stated, the physical properties of interest of the DQD array are polarization, concurrence, and probabilities for each one of the Bell states, which are calculated from the numerical solution of the stationary and dynamical equations.

The DQD array polarization is calculated as [64,70]

$$P=\frac{\eta_1+\eta_3-(\eta_2+\eta_4)}{\sum_i\eta_i}, \tag{10}$$

where η_i is the charge density in the ith quantum dot, determined from the density matrix as $\eta_i=\mathrm{Tr}(\rho_S\hat{n}_i)$. Notice that the states with charge located at opposite quantum dots, $|01\rangle$ and $|10\rangle$, correspond, respectively, to polarization $P=+1$ and -1.

In order to quantify the entanglement between the two charge qubits, we make use of Wootters' expression for concurrence [68]. For a pure state of two qubits, it is defined as

$$C=|\langle\psi|\tilde{\psi}\rangle| \tag{11}$$

with $|\tilde{\psi}\rangle=(\sigma_y\otimes\sigma_y)|\psi^*\rangle$, where σ_y is the Pauli matrix and $|\psi^*\rangle$ is the complex conjugate of $|\psi\rangle$. Thus, this expression is used for the stationary study, $|\psi\rangle$ being the ground state of the DQD array in the presence of the static potential V_a.

On the other hand, for both coherent and dissipative dynamics we employ the concurrence for a general state (pure or a mixture) of two qubits, calculated from the density matrix of the system ρ_S as [68]

$$C=\max\{0,\lambda_1-\lambda_2-\lambda_3-\lambda_4\}, \tag{12}$$

where the λ's are the square roots of the eigenvalues, in decreasing order, of the non-Hermitian matrix $\rho_S\tilde{\rho}_S=\rho_S(\sigma_y\otimes\sigma_y)\rho_S^*(\sigma_y\otimes\sigma_y)$, and ρ_S^* denotes the complex conjugation of ρ_S. The concurrence is 1 if the qubit system is maximally entangled, whereas it equals 0 when the system is separable;

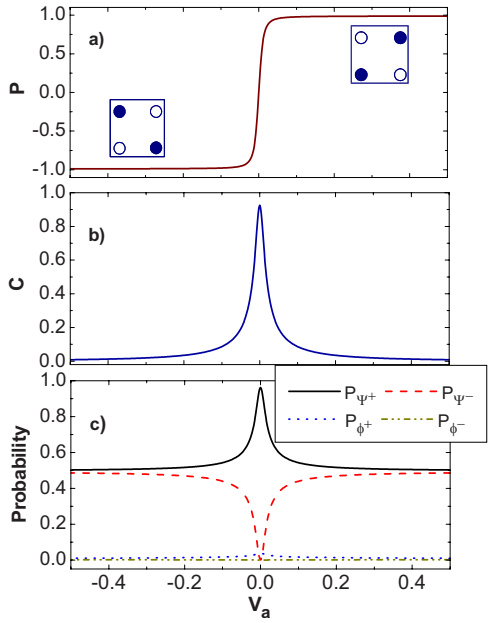

FIG. 2. (Color online) Ground state properties for the array under a static external electric field V_a: (a) polarization, (b) concurrence, and (c) Bell-state probabilities. Typical parameters used here: $t/V=0.03$, $a=100$ nm.

then Bell states have $C=1$ and each one of our basis states has null concurrence, $C=0$ [68].

Because of the largest degree of entanglement presented by the Bell states, we are interested in evaluating their contribution to the overall concurrence. By means of a basis change, a general state of the closed system can be expressed as a linear combination of Bell states as $|\psi\rangle=c_{\Psi^+}|\Psi^+\rangle+c_{\Psi^-}|\Psi^-\rangle+c_{\phi^+}|\phi^+\rangle+c_{\psi^-}|\phi^-\rangle$. One can easily find that $|\tilde{\psi}\rangle=c^*_{\Psi^+}|\Psi^+\rangle-c^*_{\Psi^-}|\Psi^-\rangle-c^*_{\phi^+}|\phi^+\rangle+c^*_{\psi^-}|\phi^-\rangle$ and then, following Eq. (11), an expression is obtained for concurrence as a function of Bell-state probabilities [57] for a pure closed system (no dissipation):

$$C=|P_{\Psi^+}-P_{\Psi^-}-P_{\phi^+}+P_{\phi^-}|, \tag{13}$$

where $P_i=|c_i|^2$ is the probability of finding the system in the ith Bell state.

III. RESULTS AND DISCUSSION

A. Stationary state

In order to characterize the basic properties of the ground state of the DQD array, in Fig. 2 we present polarization, concurrence, and Bell-state probabilities calculated as functions of the constant applied potential difference for a characteristic tunnel amplitude of $t/V=0.03$.

The polarization is shown in Fig. 2(a), where it can be observed that for negative values of V_a the ground state of the system corresponds to one where charge is mainly located on sites 2 and 4 (proportional to state $|10\rangle$). As V_a increases toward positive values, the ground state becomes that where electrons are located in an opposite configuration, that is, at sites 1 and 3 (state $|01\rangle$). This translates into a general change of polarization from $P\approx-1$ to $\approx+1$.

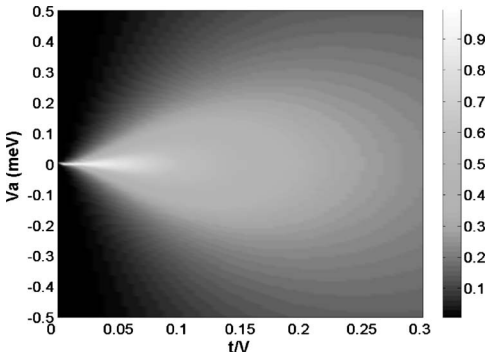

FIG. 3. Gray-scale map of stationary concurrence as a function of tunneling t/V and the constant external electric field V_a. Notice how the concurrence is adversely affected as tunneling increases, while its maximum peak becomes wider for $V_a\neq0$.

This behavior corresponds to pinning of the electron on site 2 when $V_a<0$, favoring states $|10\rangle$ and $|00\rangle$, the latter being less favorable because of electrostatic repulsion. On the other hand, when $V_a>0$, states $|01\rangle$ and $|11\rangle$ are promoted and by Coulomb interaction the $|01\rangle$ state is preferred. In the case with $V_a\approx0$, the zero polarization tells us that charge is distributed in the four QDs.

In Fig. 2(b), the concurrence as a function of the applied potential is presented, and again we find three different regimes for V_a. The concurrence starts from a very small value for $V_a<0$, growing to a maximum around $V_a\approx0$, and after this it decreases as V_a increases, reaching almost a zero value. The peak of concurrence around null V_a means that entanglement is promoted via a certain degree of charge delocalization, due to tunneling events, and as V_a increases (in absolute value) the potential tends to localize charge in almost well-defined $|01\rangle$ or $|10\rangle$ nonentangled states, in accordance with the polarization analysis.

The general behavior presented by concurrence has contributions from different Bell states. In Fig. 2(c) we observe that for both negative and positive values of V_a the states $|\Psi^+\rangle$ and $|\Psi^-\rangle$ are formed with the largest, similar probability with a very small contribution from $|\phi^+\rangle$, yielding an almost null concurrence, in agreement with Eq. (11). By exact solution of the eigenvalue problem for $V_a\approx0$, the symmetry of the square array of DQDs combined with the Coulomb interaction between electrons yield a ground state which can be written in terms of $|\Psi^+\rangle$ and $|\phi^+\rangle$ as $|\psi\rangle=\sqrt{2}\alpha|\phi^+\rangle+\sqrt{2}\beta|\Psi^+\rangle$ (with $\alpha=4t/x$, $\beta=(2-\sqrt{2}+y)/2x$, $x=\sqrt{y^2+(2-\sqrt{2})y}$ and $y=\sqrt{6-4\sqrt{2}+64t^2}$), whose concurrence can be analytically calculated from Eq. (11) or (13) as $C=2|(|\beta|^2-|\alpha|^2)|$.

For the typical tunneling used in this paper ($t/V=0.03$), $|\beta|^2>|\alpha|^2$, and then the probability of finding the system in the $|\Psi^+\rangle$ state is largest with just a minor contribution of $|\phi^+\rangle$, as shown in Fig. 2(c). This behavior is reflected in the large value for concurrence, $C=0.92$, as shown in Fig. 2(b).

We now examine tunneling effects, shown in Fig. 3, where we plot the concurrence for different values of both hopping and the external potential difference. Our results

reveal that the concurrence decreases as tunneling increases, and there is a broadening in the concurrence peak with respect to V_a. To illustrate the physical significance of this behavior, we recall the ground state for $V_a \approx 0$. In this case, transitions from $|01\rangle$ to $|10\rangle$ states (and vice versa), which give rise to the $|\Psi^+\rangle$ state, are not direct: the system can perform such transitions through population of the $|00\rangle$ and/or $|11\rangle$ states, and these processes are represented in the presence of the $|\phi^+\rangle$ state. In agreement with the previous expressions for α and β, an increment in tunneling amplitude yields a faster charge delocalization, reflected in an increment of the $|\phi^+\rangle$ probability while that of $|\Psi^+\rangle$ decreases, and, as a result, the concurrence also decreases [Eq. (13)]. Thus, tunneling and Coulomb interaction between electrons dominate the Bell state and concurrence generation for a null external potential.

On the other hand, for $V_a \neq 0$ the external potential effect is the mechanism dominating charge distribution inside the array. That means that there is a competition between charge delocalization in the QDs induced by tunneling and localization induced by the potential difference.

Note that we have considered the same tunneling amplitudes in both DQDs in order to analyze the effect of hopping in entanglement and formation of Bell states. However, we should be aware of the fact that in the experiments related to QDs it could be difficult to keep exactly the same tunneling. The generalization of our model to take it into account is straightforward. Although the dependence of entanglement on different tunnelings (say t_1 and t_2) is not trivial, in the interval $t_1/t_2=[0.3,2]$ the system follows qualitatively the same kind of behavior exhibited for equal amplitudes, as expected (not shown): there is a preferred Bell state and the concurrence is a nonmonotic curve whose maximum value, presented for a very small electric potential, depends on both the t_1 and t_2 values used. In particular, for the $V_a \sim 0$ case, it can be demonstrated that the ground state is proportional to the sum of both hopping amplitudes. As the properties of interest are not changed significantly by different tunnelings for the mentioned interval, in the next sections we consider the $t_1=t_2=t$ case for the time-dependent studies.

B. Coherent dynamics

We now examine the dynamics of the closed array of charge qubits when the external electrical field applied is linearly time dependent, $V_a(t)=-V_{a0}(t-t_0)$, and here we demonstrate that it is possible to obtain dynamical Bell states in our system by using suitable potential and nonentangled initial conditions.

The Liouville equation is solved for the time evolution of the density matrix of the system, which is used to calculate the time-dependent concurrence, the probabilities of Bell states, and the charge density on each site. As an example, in Fig. 4 we present those properties as functions of time for an initial condition corresponding to the $|01\rangle$ state for a typical tunneling amplitude of $t/V=0.03$ and $V_a(t)$ ranging from 0.375 to −0.375 meV in a time $2t_0$ (with $t_0=0.75$ ns). For longer times, $t>2t_0$, the potential becomes static, remaining at that negative value.

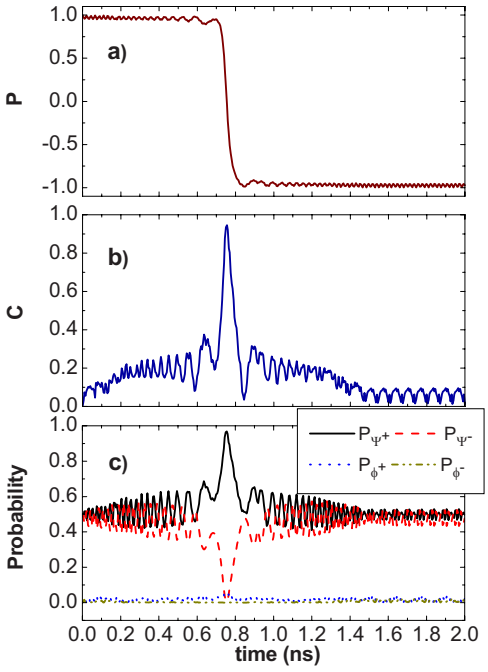

FIG. 4. (Color online) Dynamic properties when a linear time-dependent potential is applied to the second DQD. V_a takes values from 0.375 to −0.375 meV in a time $2t_0=1.5$ ns, whereas for $t>2t_0$, $V_a=-0.375$ meV. (a) Polarization, (b) concurrence, and (c) Bell-state probabilities. Again, $t/V=0.03$ and $a=100$ nm.

Figure 4(a) reveals that the initial polarization is $P \approx +1$ ($\sim|01\rangle$ state) and it is maintained in time. Then there is a switch in the polarization at times where the electric potential is around zero. For times corresponding to negative values of the external potential, the $|10\rangle$ state is favored, with $P=-1$.

In agreement with this analysis, Fig. 4(b) shows that, because the initial condition is a nonentangled state, then concurrence starts from zero and increases for low positive V_a values, presenting a peak at a time $\tau=0.75$ ns where $V_a(\tau) \approx 0$. For larger times and as this potential turns to negative values, the concurrence decreases until it vanishes when the system reaches the $|10\rangle$ state (with $P \approx -1$) as mentioned above.

The same kind of behavior is observed in the Bell-state probabilities [Fig. 4(c)], where we can notice that the system starts in a nonentangled combination of $|\Psi^+\rangle$ and $|\Psi^-\rangle$ states. Because of the effect of positive values of the electric field, the $|\Psi^+\rangle$ state is favored, yielding a peak in concurrence and a switch in polarization when $V_a(\tau) \approx 0$. Then, for larger times, the $|10\rangle \propto |\Psi^+\rangle + |\Psi^-\rangle$ nonentangled state is favored. Again, it is possible to appreciate that a certain charge delocalization induces entanglement formation from an initially separable state; thus the concurrence decreases as V_a increases in absolute value.

Notice the oscillations presented in all properties, which are due to coherence induced by tunneling between dots and the external applied potential.

For potential applications in quantum information and quantum communication, one should maintain entanglement

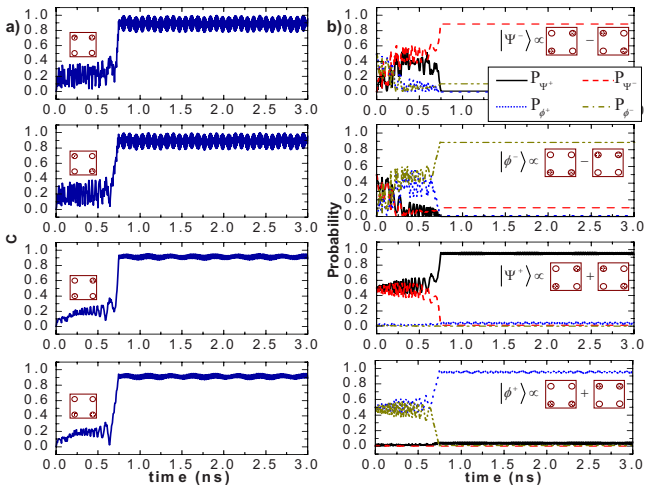

FIG. 5. (Color online) Coherent dynamics generation and control of concurrence (a) and Bell-state probabilities (b) with a linear time-dependent potential applied on the second DQD and from initial nonentangled charge distribution states: from top to bottom $|11\rangle$, $|10\rangle$, $|01\rangle$, and $|00\rangle$. Here, V_a changes linearly with time (from 0.375 to 0 meV) for $t>\tau$ and is turned off at $t\geq\tau=0.75$ ns (typical parameters as in Fig. 2).

during the whole computational process. Therefore, we turn to controlling entanglement and formation of Bell states by "removing" the potential at the time where concurrence presents a peak; that is, we let the concurrence reach its maximum value (in a characteristic time given by τ) and then it is maintained in time. To that end, we consider the same linear potential $V_a(t)=-V_{a0}(t-t_0)$ for $t<\tau$, whereas for times $t\geq\tau$ it is $V_a(t)=0$ (with the mentioned value for τ).

From now on we will refer to this driving mechanism as the *controlled* scheme, for which we show numerical results for concurrence [Fig. 5(a)] and Bell-state probabilities [Fig. 5(b)] as function of time for different initial conditions, corresponding to the four nonentangled basis states. The contributions to the concurrence from Bell states are different for each condition, depending on the time evolution of the initial charge density; however, in general, we are able to obtain just one Bell state with the largest probability in each case.

The general behavior for both concurrence and Bell-state probabilities in the presence of an external potential, $t<0.75$ ns, is in agreement with the analysis given previously for the noncontrolled case (Fig. 4). For larger times ($t\geq\tau$), we can see in Fig. 5(b), from top to bottom, that the $|\Psi^-\rangle$ state is obtained with the largest probability, which is ≈ 0.88 from the initial $|11\rangle$ state (with the electrons localized

TABLE I. Input-output truth table of the Bell states [1,10].

In	Out
$\|00\rangle$	$\|\phi^+\rangle=(\|00\rangle+\|11\rangle)/\sqrt{2}$
$\|01\rangle$	$\|\Psi^+\rangle=(\|01\rangle+\|10\rangle)/\sqrt{2}$
$\|10\rangle$	$\|\phi^-\rangle=(\|00\rangle-\|11\rangle)/\sqrt{2}$
$\|11\rangle$	$\|\Psi^-\rangle=(\|01\rangle-\|10\rangle)/\sqrt{2}$

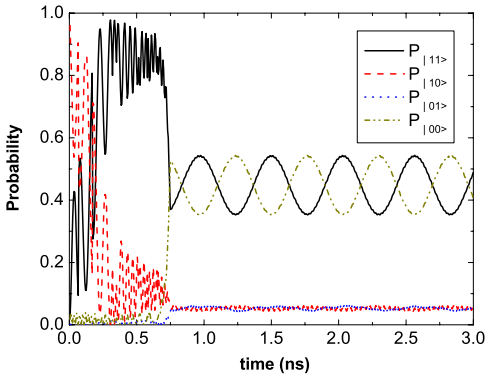

FIG. 6. (Color online) Time-dependent probabilities of the basis states for the controlled potential scheme. Initial condition $|10\rangle$ state (typical parameters for t/V and a).

in the top of both DQDs). The initial $|10\rangle$ state, where the charge is localized in the second and fourth QDs, yields the $|\phi^-\rangle$ state with a probability around 0.88, whereas from the opposite charge distribution state, $|01\rangle$, it is possible to obtain $|\Psi^+\rangle$ with probability 0.95. Finally, the initial $|00\rangle$ state, which corresponds to the electrons localized at the bottom of the DQD array, generates the $|\phi^+\rangle$ state with probability around 0.95. In the four cases, the corresponding concurrence is oscillating around 0.9.

This mechanism for generation of Bell states is in agreement with the theoretical quantum "truth table" proposed for the same purpose [1,10], as shown in Table I.

In order to understand the mechanism involved in such generation of Bell states, the time evolution of the probability for the basis states is analyzed. As examples, Figs. 6 and 7 show the behavior for $|10\rangle$ and $|01\rangle$ initial conditions, respectively. For the first case, we can observe how the probability for the $|10\rangle$ state decreases while that for the $|11\rangle$ state grows, in the interval $0<t<0.2$ ns. For times $t\approx 0.2$ ns, the probability of $|11\rangle$ exceeds that of $|10\rangle$, and when the electric external potential is removed the system remains oscillating coherently between the $|00\rangle$ and $|11\rangle$ states (in a kind of Rabi oscillation between two states), resulting in the $|\phi^-\rangle$ state. The inverse behavior is presented when we use the initial $|11\rangle$ state, yielding the formation of $|\Psi^-\rangle$ (not shown).

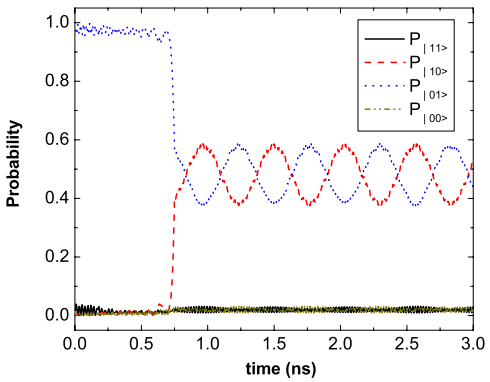

FIG. 7. (Color online) Time-dependent probabilities of the basis states for the controlled potential scheme. Initial condition $|01\rangle$ state and the same parameters as in Fig. 6.

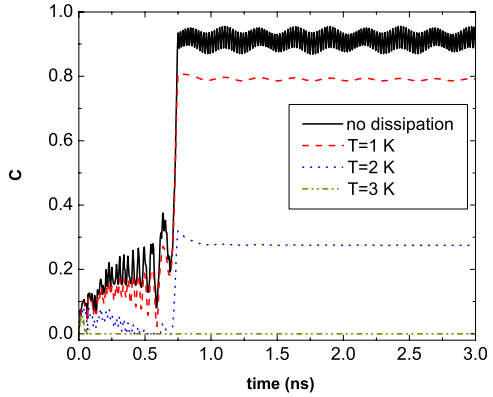

FIG. 8. (Color online) Time-dependent concurrence including dissipation effects for the controlled potential scheme. The concurrence presents large values for very low temperature but deteriorates as temperature increases (parameters $t/V=0.03$, $a=100$ nm, and $D^2=0.005$).

On the other hand, for the initial condition given by the $|01\rangle$ state (Fig. 7), the system remains in that state with the largest probability for $0<t<0.75$ ns, and when V_a is removed the probability of the $|10\rangle$ state grows. Then the system charge oscillates among such configurations, giving rise to the $|\Psi^+\rangle$ state. A similar dynamics is obtained by using the initial $|00\rangle$ state, which gives rise to a coherent combination of $|00\rangle$ and $|11\rangle$ states and thus to the $|\phi^+\rangle$ state (not shown).

From this discussion, we observe that the dynamics of the system at the time $t\approx 0.2$ ns exhibits a behavior which corresponds with the result of a controlled-NOT (CNOT) operation. In a similar way, for $t\approx\tau$ the dynamics is consistent with the result of a Z gate applied on the first qubit plus an X gate performed on both qubits. That means that the electrostatic mechanism analyzed here has induced an operation proportional to $(Z\otimes I+X\otimes X)$ CNOT over the two-charge-qubit system, which can be proved to be equivalent to the theoretical proposed circuit to create the Bell states, CNOT $(H\otimes I)$, where H is the Hadamard gate [1,9,10].

One should bear in mind that, although the initial polarization is well defined for each initial condition, the controlled scheme refers to the states where the system has reached its maximal concurrence with $V_a(t)=0$, corresponding to zero polarization for each case. Therefore, this property is not shown here.

C. Dissipative dynamics

In the controlled scheme for the generation of entanglement and Bell states, we evaluate the effect of the phonon environment on the DQD array properties, presented in Figs. 8 and 9 for an initial $|01\rangle$ state.

The time-dependent concurrence for different temperatures is presented in Fig. 8, where we observe that it shows a large value $(C\approx 0.8)$ for the very low temperature of $T=1$ K, but deteriorates as the temperature increases until the charge qubits become completely uncorrelated.

In accordance with Eq. (8) the transition rates between the states become equally probable as temperature increases, due to the interaction with the thermal bath. This results in similar electron probabilities in each QD and consequently a faster depolarization of the DQD array (not shown) and the loss of a preferred Bell state. In Fig. 9(a) it is shown that, for times longer than τ, the probability of the $|\Psi^+\rangle$ state decreases from $P_{\Psi^+}\approx 0.95$ for the closed system (no dissipation) down to $P_{\Psi^+}\approx 0.47$ for $T=3$ K, whereas those for the $|\Psi^-\rangle$, $|\phi^+\rangle$, and $|\phi^-\rangle$ states increase from almost zero in the closed case to $P_{\Psi^-}\approx 0.23$, $P_{\phi^+}\approx 0.15$, and $P_{\phi^+}\approx 0.15$ for $T=3$ K [Figs. 9(b)–9(d)].

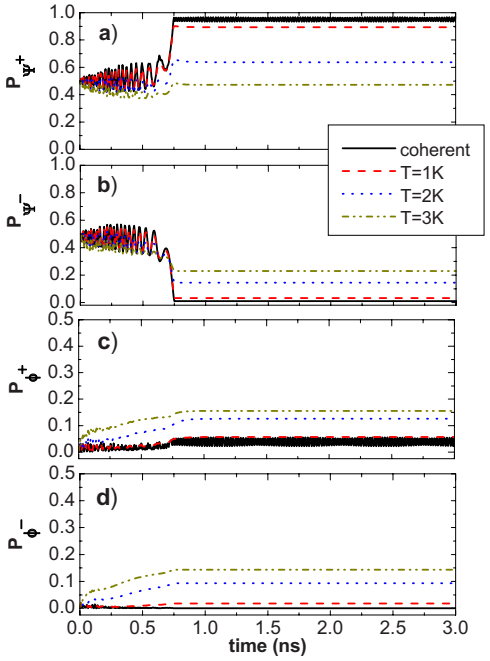

FIG. 9. (Color online) Temperature effects on time evolution of Bell-state probabilities yielding mixed states with decreasing concurrence. The external potential ranges from 0.375 to 0 meV in a time τ (same parameters as in Fig. 8).

The oscillations of concurrence and Bell-state probabilities also decrease with increasing temperature due to the decay of the coherent terms in the density matrix Eq. (6).

For times much longer than τ, the system reaches a stationary state which does not depend on the initial condition. As tunneling is an important parameter for charge distribution in the absence of the external potential, in Fig. 10 we present the asymptotic (or long-time) concurrence as a function of temperature for different hopping amplitudes and for the controlled scheme. Our results show that concurrence decreases as tunneling increases; however, it exhibits large values for very low temperatures $T<1$ K, presenting a rapid decay as temperature increases and vanishing at a critical or threshold temperature T_c, which also increases as tunneling increases. For the typical hopping used here $(t/V=0.03)$, we found $T_c=2.78$ K.

The asymptotic concurrence behavior reveals that tunneling is the dominant mechanism contributing to entanglement formation in the low-temperature regime. On the other hand, the general nature of concurrence for long times and $T>T_c$ can be physically understood if we bear in mind that bath equilibration processes yield an equal population in each

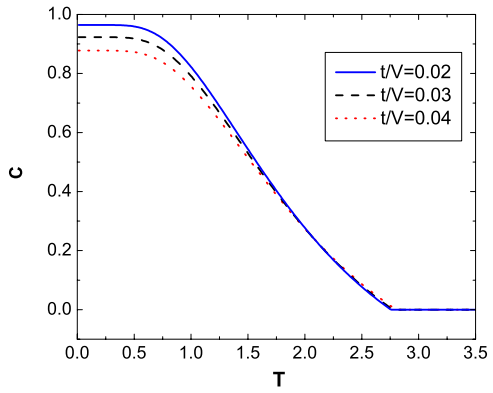

FIG. 10. (Color online) Asymptotic behavior of concurrence as a function of temperature for different tunneling amplitudes. There is a critical temperature T_c at which concurrence vanishes, which also depends on tunneling. For the hopping values shown here, it is in the interval $2.5 < T_c < 3$ K.

QD, such that the reduced density matrix is diagonal and all the eigenvalues of $\rho_S \tilde{\rho}_S$ are equal. Then, by definition, Eq. (12), the concurrence is zero for finite temperature, in agreement with Ref. [74].

IV. CONCLUSION

We have demonstrated that entanglement and generation of Bell states between two charge qubits, represented by the charge degree of freedom of two parallel coupled quantum dots, can be dynamically obtained and coherently controlled by an external electric field. By properly choosing uncorrelated initial conditions and a time-dependent driver potential, we can dynamically obtain each one of the four Bell states with the largest probability in the system.

We have also considered dissipation effects by studying the role of temperature in the time evolution of the density matrix of the system when the charge-qubit array is coupled to a thermal bath of phonons (by means of the nondiagonal electron-phonon interaction). It is found that optimal concurrence and probabilities are maintained at very low temperature, but are adversely affected by increasing temperatures. Concurrence between the qubits vanishes for a finite temperature that depends on the tunneling amplitude ($T_c = 2.78$ K for the typical hopping used here).

This electric mechanism for entanglement and generation of Bell states could be of interest in future quantum-gate and quantum-information and -computation implementations, where the ability to manipulate such Bell states and/or the temperature could be feasible.

ACKNOWLEDGMENTS

We would like to acknowledge R. Aguado for helpful comments and also E. Cota for fruitful discussions and for his critical reading of the paper. The work was supported in part by DGAPA (Project No. IN114403) and by CONACyT (Project No. 43673-F).

[1] M. A. Nielsen and I. L. Chuang, *Quantum Computation and Quantum Information* (Cambridge University Press, Cambridge, U.K., 2000).
[2] G. Vidal and R. F. Werner, Phys. Rev. A **65**, 032314 (2002).
[3] G. Burkard, D. Loss, and D. P. DiVincenzo, Phys. Rev. B **59**, 2070 (1999).
[4] D. Loss and D. P. DiVincenzo, Phys. Rev. A **57**, 120 (1998).
[5] C. H. Bennett, H. J. Bernstein, S. Popescu, and B. Schumacher, Phys. Rev. A **53**, 2046 (1996).
[6] B. Schumacher, Phys. Rev. A **51**, 2738 (1995).
[7] F. Mintert, A. R. R. Carvalho, M. Kuś, and A. Buchleitner, Phys. Rep. **415**, 207 (2005).
[8] M. Brooks, in *Quantum Computing and Communications*, edited by M. Brooks (Springer, London, 1999).
[9] G. Blatter, Nature (London) **421**, 796 (2003).
[10] http://www.theory.caltech.edu/people/preskill/ph229.
[11] C. H. Bennett, G. Brassard, C. Crépeau, R. Jozsa, A. Peres, and W. K. Wootters, Phys. Rev. Lett. **70**, 1895 (1993).
[12] D. Bouwmeester, J. W. Pan, K. Mattle, M. Eibl, H. Weinfurter, and A. Zeilinger, Nature (London) **390**, 575 (1997).
[13] C. H. Bennett and S. J. Wiesner, Phys. Rev. Lett. **69**, 2881 (1992).
[14] S. Popescu and D. Rohrlich, in *Introduction to Quantum Computation and Information*, edited by H.-K. Lo, S. Popescu, and T. Spiller (World Scientific, Singapore, 1998).
[15] D. Bouwmeester and A. Zeilinger, in *The Physics of Quantum Information*, edited by D. Bouwmeester, A. Ekert, and A. Zeilinger (Springer, Berlin, 2000).
[16] D. Deutsch, Proc. R. Soc. London, Ser. A **425**, 73 (1985).
[17] Y. H. Kim, S. P. Kulik, M. V. Chekhova, W. P. Grice, and Y. Shih, Phys. Rev. A **67**, 010301(R) (2003).
[18] T. E. Keller, M. H. Rubin, Y. Shih, and L.-A. Wu, Phys. Rev. A **57**, 2076 (1998).
[19] P. I. Tamborenea and H. Metiu, Europhys. Lett. **53**, 776 (2001).
[20] A. Steane, Rep. Prog. Phys. **61**, 117 (1998).
[21] L. Quiroga and N. F. Johnson, Phys. Rev. Lett. **83**, 2270 (1999).
[22] C. F. Roos, G. P. T. Lancaster, M. Riebe, H. Häffner, W. Hansel, S. Gulde, C. Becher, J. Eschner, F. Schmidt-Kaler, and R. Blatt, Phys. Rev. Lett. **92**, 220402 (2004).
[23] M. Riebe, H. Häffner, C. F. Roos, W. Hansel, J. Benhelm, G. P. T. Lancaster, T. W. Korber, C. Becher, F. Schmidt-Kaler, D. F. V. James, and R. Blatt, Nature (London) **429**, 734 (2004); M. D. Barrett, J. Chiaverini, T. Schaetz, J. Britton, W. M. Itano, J. D. Jost, E. Knill, C. Langer, D. Leibfried, R. Ozeri, and D. J. Wineland, *ibid.* **429**, 737 (2004).
[24] H. Häffner, F. Schmidt-Kaler, W. Hänsel, C. Roos, T. Körber, M. Riebe, J. Benhelm, U. Rapol, C. Becher, and R. Blatt, Appl. Phys. B: Lasers Opt. **81**, 151 (2005).
[25] K. J. Resch, J. S. Lundeen, and A. M. Steinberg, J. Quantum Comput. Comput. **4**, 81 (2003).

[26] D. Fattal, K. Inoue, J. Vuckovic, C. Santori, G. S. Solomon, and Y. Yamamoto, Phys. Rev. Lett. **92**, 037903 (2004).
[27] Y.-H. Kim, M. V. Chekhova, S. P. Kulik, M. H. Rubin, and Y. Shih, Phys. Rev. A **63**, 062301 (2001).
[28] R. García-Maraver, R. Corbalán, K. Eckert, S. Rebic, M. Artoni, and J. Mompart, Phys. Rev. A **70**, 062324 (2004).
[29] B. B. Blinov, D. L. Moehring, L. M. Duan, and C. Monroe, Nature (London) **428**, 153 (2004).
[30] A. Messina, Eur. Phys. J. D **18**, 379 (2002).
[31] L. Davidovich, N. Zagury, M. Brune, J. M. Raimond, and S. Haroche, Phys. Rev. A **50**, R895 (1994).
[32] A. Ekert and R. Jozsa, Rev. Mod. Phys. **68**, 733 (1996).
[33] A. Imamoglu, D. D. Awschalom, G. Burkard, D. P. DiVincenzo, D. Loss, M. Sherwin, and A. Small, Phys. Rev. Lett. **83**, 4204 (1999).
[34] Z. J. Wu, K. D. Zhu, X. Z. Yuan, Y. W. Jiang, and H. Zheng, Phys. Rev. B **71**, 205323 (2005).
[35] S. Vorojtsov, E. R. Mucciolo, and H. U. Baranger, Phys. Rev. B **71**, 205322 (2005).
[36] J. R. Petta, A. C. Johnson, J. M. Taylor, E. A. Laird, A. Yacoby, M. D. Lukin, C. M. Marcus, M. P. Hanson, and A. C. Gossard, Science **309**, 2180 (2005).
[37] P. Zhang, Q.-K. Xue, X. G. Zhao, and X. C. Xie, Phys. Rev. A **66**, 022117 (2002).
[38] S. Weiss, M. Thorwart, and R. Egger, Europhys. Lett. **76**, 905 (2006).
[39] L. P. Kouwenhoven *et al.*, in *Mesoscopic Electron Transport*, NATO ASI, Ser. E: Applied Sciences, edited by L. L. Sohn, L. P. Kouwenhoven and G. Schön (Kluwer, Dordrecht, 1997), Vol. 345.
[40] W. G. van der Wiel, S. de Franceschi, J. M. Elzerman, T. Fujisawa, S. Tarucha, and L. P. Kouwenhoven, Rev. Mod. Phys. **75**, 1283 (2003).
[41] W. G. van der Wiel, T. Fujisawa, S. Tarucha, and L. P. Kouwenhoven, Jpn. J. Appl. Phys., Part 1 **40**, 2100 (2001).
[42] W. B. Chouikha, S. Jaziri, and R. Bennaceur, J. Supercond. **16**, 313 (2003).
[43] J. M. Elzerman, R. Hanson, J. S. Greidanus, L. H. Willems van Beveren, S. de Franceschi, L. M. K. Vandersypen, S. Tarucha, and L. P. Kouwenhoven, Phys. Rev. B **67**, 161308(R) (2003).
[44] J. R. Petta, A. C. Johnson, C. M. Marcus, M. P. Hanson, and A. C. Gossard, Phys. Rev. Lett. **93**, 186802 (2004).
[45] J. Gorman, D. G. Hasko, and D. A. Williams, Phys. Rev. Lett. **95**, 090502 (2005).
[46] T. Hayashi, T. Fujisawa, H. D. Cheong, Y. H. Jeong, and Y. Hirayama, Phys. Rev. Lett. **91**, 226804 (2003).
[47] T. Fujisawa, T. Hayashi, and Y. Hirayama, J. Vac. Sci. Technol. B **22**, 2035 (2004).
[48] W. A. Coish and D. Loss, Phys. Rev. B **72**, 125337 (2005).
[49] T. Tanamoto, Phys. Rev. A **61**, 022305 (2000).
[50] T. Tanamoto and X. Hu, J. Phys.: Condens. Matter **17**, 6895 (2005).
[51] P. Zanardi and F. Rossi, Phys. Rev. Lett. **81**, 4752 (1998).
[52] G. Chen, N. H. Bonadeo, D. G. Steel, D. Gammon, D. S. Katzer, D. Park, and L. J. Sham, Science **289**, 1906 (2000).
[53] X. X. Yi, G. R. Jin, and D. L. Zhou, Phys. Rev. A **63**, 062307 (2001).
[54] A. Hichri, S. Jaziri, and R. Ferreira, Phys. Status Solidi C **1**, 598 (2004).
[55] J. H. Reina, L. Quiroga, and N. F. Johnson, Phys. Rev. A **62**, 012305 (2000).
[56] R. Roloff and W. Pötz, Phys. Rev. B **76**, 075333 (2007).
[57] L. D. Contreras-Pulido and F. Rojas, J. Phys.: Condens. Matter **18**, 9771 (2006).
[58] J. Kyriakidis, M. Pioro-Ladriere, M. Ciorga, A. S. Sachrajda, and P. Hawrylak, Phys. Rev. B **66**, 035320 (2002).
[59] T. A. Costi and R. H. McKenzie, Phys. Rev. A **68**, 034301 (2003).
[60] M. Thorwart, E. Paladino, and M. Grifoni, Chem. Phys. **296**, 333 (2004).
[61] T. Brandes, Phys. Rep. **408**, 315 (2005).
[62] U. Weiss, *Quantum Dissipative Systems* (World Scientific, Singapore, 1999).
[63] A. J. Leggett, S. Chakravarty, A. T. Dorsey, M. P. A. Fisher, A. Garg, and W. Zwerger, Rev. Mod. Phys. **59**, 1 (1987).
[64] C. K. Wang, I. I. Yakimenko, K. F. Berggren, and I. V. Zozoulenko, J. Appl. Phys. **84**, 2684 (1998).
[65] A. Y. Smirnov, N. J. M. Horing, and L. G. Mourokh, J. Appl. Phys. **87**, 4525 (2000).
[66] E. Cota, F. Rojas, and S. E. Ulloa, Phys. Status Solidi B **230**, 377 (2002) b.
[67] F. Rojas, E. Cota, and S. E. Ulloa, Phys. Rev. B **66**, 235305 (2002).
[68] W. K. Wootters, Phys. Rev. Lett. **80**, 2245 (1998).
[69] G. Shinkai, T. Hayashi, Y. Hirayama, and T. Fujisawa, Appl. Phys. Lett. **90**, 103116 (2007).
[70] C. S. Lent, P. D. Tougaw, W. Porod, and G. H. Bernstein, Nanotechnology **4**, 49 (1993); C. S. Lent and P. Tougaw, J. Appl. Phys. **75**, 4077 (1994).
[71] See, for example, C. Kittel, *Quantum Theory of Solids* (John Wiley & Sons, New York, 1987); J. H. Davies, *The Physics of Low-Dimensional Semiconductors: An Introduction* (Cambridge University Press, Cambridge, U.K., 1998); P. Y. Yu and M. Cardona, *Fundamentals of Semiconductors: Physics and Materials Properties* (Springer, Berlin, 1996); J. Bardeen and W. Shockley, Phys. Rev. **80**, 72 (1950).
[72] K. Blum, *Density Matrix Theory and Applications* (Plenum Press, New York, 1981).
[73] G. Mahler and V. A. Weberruß, *Quantum Networks: Dynamics of Open Nanostructures* (Springer-Verlag, Berlin, 1995).
[74] B. V. Fine, F. Mintert, and A. Buchleitner, Phys. Rev. B **71**, 153105 (2005).